chem) on glass slides and viewed and photographed with a Nikon Optiphot photomicroscope. Omission of primary antiserum or its replacement with non- or preimmune serum resulted in no detectable staining.
9. U. Lendahl, L. B. Zimmerman, R. D. G. McKay, *Cell* **60**, 585 (1990); K. Frederiksen and R. D. G. McKay, *J. Neurosci.* **8**, 144 (1988).
0. B. A. Reynolds and S. Weiss, unpublished data.
.1. After 6 DIV, spheres were transferred with wide-bore pipettes into a test tube and mechanically dissociated into single cells with a fire-narrowed Pasteur pipette. Single cells were plated (by limiting dilution of the cell suspension) into the bases of 96-well culture dishes containing serum-free medium plus EGF. The presence of a single cell in a well was confirmed with phase-contrast microscopy and photography with a Nikon Diaphot inverted photomicroscope.
12. A. M. Graybiel, *Trends Neurosci.* **13**, 244 (1990).
13. Although these antisera did not label any cells in the EGF-generated cultures, we have successfully used them to identify discrete populations of neurons in cultures of embryonic mouse cortex, hippocampus, ventral mesencephalon (unpublished observations), and striatum [J. H. Williams, I. Berbekar, S. Weiss, *Neuroscience* **43**, 437 (1991)].
14. C. M. Morshead and D. van der Kooy, *J. Neurosci.* **12**, 249 (1992).
15. J. C. Fentress, B. B. Stanfield, W. M. Cowan, *Anat. Embryol.* **163**, 275 (1981).
16. E. Cattaneo and R. McKay, *Trends Neurosci.* **14**, 338 (1991).
17. A. R. Kay and R. K. S. Wong, *J. Neurosci. Methods* **16**, 227 (1986).
18. S. Weiss *et al.*, *Proc. Natl. Acad. Sci. U.S.A.* **83**, 2238 (1986).
19. Supported by the Medical Research Council (MRC) of Canada. B.A.R. is a recipient of a Pharmaceutical Manufacturers Association of Canada–MRC studentship; S.W. is an MRC Scholar. We thank W. Tetzlaff for advice and discussion; A. G. M. Bulloch, R. Hawkes, and A. Vescovi for helpful comments; D. D. Fraser and B. A. MacVicar for advice on dissociation procedures; M. Marvin and R. McKay for antisera to nestin; and S. Pleasure and V. Lee for antibody to neurofilament.

23 December 1991; accepted 28 January 1992

Evidence for a Computational Distinction Between Proximal and Distal Neuronal Inhibition

ERIC T. VU*† AND FRANKLIN B. KRASNE

Most neurons have inhibitory synapses both "proximally" near the spike-initiating zone and "distally" on dendrites. Although distal inhibition is thought to be an adaptation for selective inhibition of particular dendritic branches, another important distinction exists between proximal and distal inhibition. Proximal inhibition can attenuate excitatory input absolutely so that no amount of excitation causes firing. Distal inhibition, however, inhibits relatively; any amount of it can be overcome by sufficient excitation. These properties are used as predicted in the circuit-mediating crayfish escape behavior. Many neuronal computations require relative inhibition. This could partly account for the ubiquity of distal inhibition.

MOST CENTRAL NEURONS RECEIVE inhibitory inputs on their basal dendrites or somata, where they are well situated to shunt distally generated excitatory postsynaptic potentials (EPSPs) before they spread to the axonal spike initiating zone. Such "proximal inhibition" was discovered first, but it is now known that distal dendrites also commonly receive extensive inhibitory as well as excitatory inputs (*1*). A reason often proposed for such "distal inhibition" is that it would allow for selective inhibition of particular dendritic branches (*2*). While studying inhibitory control of the lateral giant (LG) command neurons for crayfish tail-flip escape behavior, we have come to appreciate a different and perhaps more generally important reason for distal inhibition.

Neuroscience Program, Department of Psychology, and the Brain Research Institute, University of California, Los Angeles, CA 90024.

*To whom correspondence should be addressed.
†Present address: Division of Biology 216-76, California Institute of Technology, Pasadena, CA 91125.

Two kinds of suppression of LG escapes are known: (i) Escape cannot be initiated while an escape response is in progress. The responsible suppressive influence is called recurrent inhibition (*3*). Because initiating a new response while another is in progress would be maladaptive, recurrent inhibition should be absolute: No matter how strong the provocation, the inhibition should prevent a response. (ii) The likelihood of escape is reduced when crayfish are feeding or are restrained so that escape would be ineffectual (*4*). The responsible process, tonic inhibition, is strategic in nature: Although ignoring a modest threat to continue feeding may be adaptive, sufficient provocation should still cause escape. Thus, it should be possible to override tonic inhibition.

Both recurrent and tonic inhibition are known to be directed to the LG neuron itself and thus might be produced by the same inhibitory neurons. However, a consideration of the way excitation and inhibition interact suggests that proximal inhibition best confers the absolute suppression required for recurrent inhibition, whereas distal inhibition can more readily be overcome by strong excitation, as required for tonic inhibition.

The reason is illustrated in Fig. 1, which shows predictions from a steady-state, two-compartment model of LG (equivalent circuit insets). Attenuation of EPSPs from distal to proximal compartment was by a factor of 10, consistent with known physiology and anatomy. The top curve in Fig. 1, A1 and A2, shows the depolarization produced by excitation in the absence of inhibition. Depolarization increases with increasing excitation until the EPSP at its distal origin approaches the excitatory synaptic reversal potential and saturates. Thus, the curve plateaus.

Proximal inhibition decreases EPSP amplitude by a nearly constant factor independent of the amount of excitation (Fig. 1, A1 and B1). Thus, if the inhibitory strength were sufficient to reduce the plateau of the curve in Fig. 1, A1, below the critical firing level of the proximal compartment (for example, the dashed line), then no amount of additional excitation would fire the cell. In other words, the inhibition would be absolute, as required for recurrent inhibition.

Distal inhibition behaves differently. Because it reduces EPSPs in the distal compartment itself, it tends to counter the excitatory saturation, allowing excitatory levels that in the uninhibited situation would produce no further potential change to do so, until the inhibition is overcome and excitation again saturates. Thus, any amount of distal inhibition can be overcome by further excitation, as reflected in Fig. 1, A2, by the fact that all curves crossed the critical firing level with strong enough excitation. Consequently, distal inhibition can be overridden, as required for tonic inhibition. We refer to the different functional properties of inhibition conferred by proximal and distal synapses as "absoluteness" and "relativity," respectively.

These arguments imply that recurrent inhibition of LG should operate proximally, whereas tonic inhibition should be distal. Is this the case? To evaluate this, we compared the conductance increases produced by recurrent and tonic inhibition in the proximal dendrites of LG (Fig. 2A). If the hypothesis is correct, the proximal conductance increase associated with recurrent inhibition should be much greater than that associated with comparable amounts of tonic inhibition.

Recurrent inhibition was produced by firing the medial giant neurons, which cause an escape response without LG neuron involvement (*5*); inhibition was measured near its maximum, about 10 ms after medial giant firing (*3*) (Fig. 2, B1). We measured recurrent inhibition in the absence of tonic inhibition by isolating the abdominal ner-

vous system, where the LG dendrites are located, from rostral neural centers, where tonic inhibition originates (*4*). Intact animals (*6*) prepared for intracellular recording tend to tonically inhibit escape, because the necessary restraint reliably evokes such inhibition. We reversibly removed the effects of tonic inhibition by blocking conduction into the abdomen with a sucrose block of descending fibers (*7*). B2 and B3 in Fig. 2 show how sucrose block disinhibited EPSPs in LG produced by a brief shock to a sensory root (*8*).

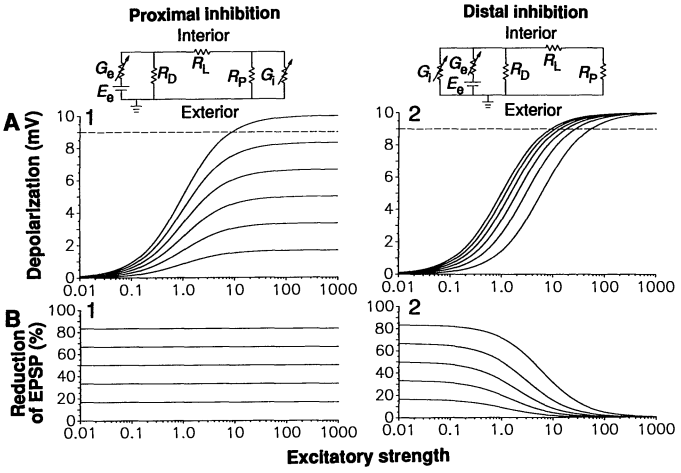

Fig. 1. Computational distinction between proximal and distal inhibition. (**A**) Proximally measured steady-state EPSP amplitudes as a function of strength of distal excitation, with inhibition modeled by proximal (1) or distal (2) conductances, G_i's (insets). Curves were generated with increasing values of G_i/G_D (0 for top curve, 0.2, 0.5, 1, 2, 5 for successively lower curves; $G_D = 1/R_D$). Excitation is modeled by the variable conductance G_e and driving potential E_e (100 mV) (*14*). Proximal and distal compartmental resistances are R_P and R_D; R_L = longitudinal resistance. Curves were generated with $R_P/(R_P + R_L) = 0.1$ and $R_P = R_D$. Abscissa values given as the ratio G_e/G_D. The electrochemical batteries for resting and inhibitory reversal potentials were not included and assumed to be close in value. (**B**) Percentage reductions of EPSPs for the inhibition curves in (A).

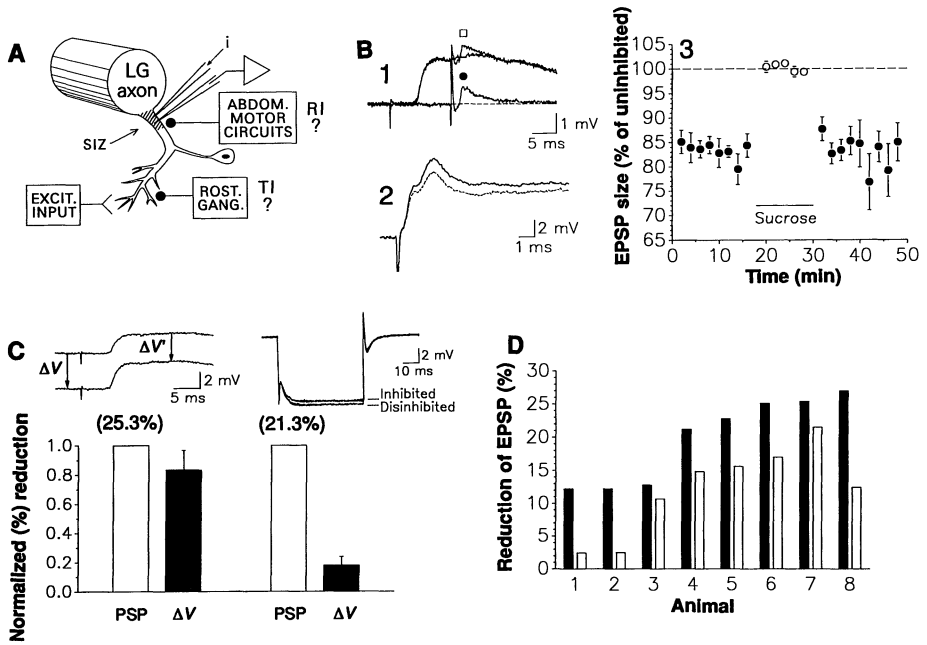

Fig. 2. Proximal and distal inhibition of LG. (**A**) Sensory circuitry (excit. input) excites the LG dendrites distantly from the neuron's spike-initiating zone (SIZ, hatched), where microelectrodes were placed (i, injected current). Postulated input sites of recurrent inhibition (RI, from abdominal motor circuits) and tonic inhibition (TI, from rostral ganglia) are indicated. (**B**) (1) Recurrent inhibition. Three traces are superimposed: (i) EPSP evoked by firing an identified sensory interneuron (dot above trace), (ii) larger, depolarizing IPSP due to recurrent inhibition, and (iii) attenuated EPSP (square) on the IPSP plateau. (2) EPSP evoked by shocking sensory root (downward deflection). The upper trace was recorded during sucrose block of TI and the lower before block. (3) Normalized size of EPSP as in (2) pooled from four animals. (**C**) Comparison of percent reductions of conductance (assessed proximally) and EPSPs for recurrent (left) and tonic inhibition (right). For each inhibition type, values are expressed relative to the percentage EPSP reduction (actual mean EPSP reductions in parentheses). Sample traces are shown above their respective data. For recurrent inhibition, hyperpolarizing currents were injected, and ΔV was assessed with and without the recurrent IPSP (reduction = $(\Delta V - \Delta V')/\Delta V$). For tonic inhibition, three inhibited and three uninhibited traces are superimposed. (**D**) Attenuation of small and large EPSPs by tonic inhibition. Solid bars are for small EPSPs, and unfilled bars are for large EPSPs in the same animals.

In these experiments, tonic inhibition and recurrent inhibition were roughly commensurate in magnitude, both reducing distally originating EPSPs by 20 to 30%. We evaluated the conductance near the proximal electrode impalement site by measuring the voltage shift (ΔV) produced by injecting a constant current pulse through a second microelectrode (Fig. 2C) (ΔV is then inversely proportional to local conductance). Our hypothesis predicts that for commensurate amounts of inhibition, ΔV should be reduced more by recurrent than by tonic inhibition. Figure 2C shows that this was the case. Consistent with previous work (*9*), recurrent inhibition reduced ΔV by almost as much as it did EPSPs, suggesting that the associated conductance increase was located near the electrode impalement site, while tonic inhibition reduced ΔV only slightly, though measurably. The average ratio of ΔV reduction to EPSP reduction was 0.834 (0.234 SD) for recurrent and 0.179 (0.136 SD) for tonic inhibition ($t_6 = 5.13$, where 6 is the sample size; $P < 0.01$) (*10*).

Both inhibitions were associated with small depolarizing, γ-aminobutyric acid (GABA)–mediated inhibitory postsynaptic potentials (IPSPs). However, as seen at the proximal recording site, the average recurrent IPSP was 2.41 mV (0.41 SD), whereas the tonic IPSP was 0.44 mV (0.19 SD).

Another prediction from our hypothesis is that the EPSP attenuation produced by proximal inhibition should be largely independent of EPSP amplitude, whereas distal inhibition should attenuate small EPSPs more than large ones (compare Fig. 1, B1 and B2). To test this, we compared tonic inhibition of small (average peak of 3.8 mV) and large (6.1 mV) EPSPs in the same preparation for eight animals. The smaller EPSP was in fact always inhibited more strongly (Fig. 2D) (20% mean reduction for small EPSPs, 12% for large EPSPs; $t_7 = 5.67$; $P < 0.001$) (*11*).

These observations provide evidence that the theoretical difference between proximal and distal inhibition (Fig. 1) is utilized by the organism. This could be established for the LG neuron because the behavioral consequences of the inhibitory events were known, but it seems likely that this difference is exploited rather generally.

The distinction between proximal and distal inhibition may also be seen in their differing effects on repetitive firing to sustained input (*12*). Proximal inhibition will tend to reduce the maximum firing rate of

the cell, whereas distal inhibition will make the cell less responsive but still able to fire at its highest uninhibited rate when stimulated more strongly. In essence, the dynamic range of the cell is reduced by proximal but unaffected by distal inhibition.

Thus, when computational requirements dictate that inhibition be absolute, we would expect proximally placed inhibitory synapses. In contrast, when it is necessary that inhibition be overridden by sufficient excitation or when it is necessary to decrease the responsiveness of a neuron without reducing its dynamic range, distal inhibition should be used. Many computations performed by neural circuits must require inhibition that is relative (*13*). We suggest that this may be a major reason for the ubiquity of distal inhibition in higher nervous systems.

REFERENCES AND NOTES

1. R. Llinas and C. Nicholson, *J. Neurophysiol.* **34**, 532 (1971); Y. Fujita, *Brain Res.* **175**, 59 (1979); K. Mori *et al.*, *J. Neurosci.* **9**, 2291 (1984).
2. W. Rall, in *Neural Theory and Modeling*, R. F. Reiss, Ed. (Stanford Univ. Press, Palo Alto, CA, 1964), pp. 73–97; R. Llinas, in *Advances in Neurology*, G. W. Kreutzberg, Ed. (Raven, New York, 1975), vol. 12, pp. 1–13; J. J. B. Jack, D. Noble, R. W. Tsien, *Electric Current Flow in Excitable Cells* (Oxford Univ. Press, New York, 1975), pp. 197–213; G. M. Shepherd and C. Koch, in *The Synaptic Organization of the Brain*, G. M. Shepherd, Ed. (Oxford Univ. Press, New York, ed. 3, 1990), pp. 439–473.
3. A. Roberts, *J. Exp. Biol.* **48**, 545 (1968).
4. F. B. Krasne and J. J. Wine, *ibid.* **63**, 433 (1975); F. B. Krasne and S. C. Lee, *J. Neurosci.* **8**, 3703 (1988).
5. J. J. Wine and F. B. Krasne, *J. Exp. Biol.* **56**, 1 (1972).
6. Crayfish (*Procambarus clarkii*) were anesthetized by cooling, then their hemolymph was replaced with cold, aerated Ringer solution [A. van Harreveld, *Proc. Soc. Exp. Biol. Med.* **34**, 428 (1936)] to prevent clotting.
7. A connective between two abdominal ganglia was isolated from the circulating Ringer solution by a chamber in which Ringer and an isotonic sucrose solution could be exchanged.
8. Shocking the second ganglionic root recruits mechanosensory fibers that excite LG both mono- and disynaptically via a pool of interneurons [F. B. Krasne, *J. Exp. Biol.* **50**, 29 (1969)]. Recurrent inhibition reduced the monosynaptic component of root-evoked EPSPs by the same amount as the EPSP in Fig. 2, B1, but reduced the disynaptic component more because of additional inhibition at the first synapse of the circuit.
9. Data from (*3*) provide a value of 0.788 for the relative reductions of ΔV and EPSPs.
10. Tonic inhibition is largely if not wholly due to postsynaptic inhibition: it substantially shunts current passed between the bilateral LGs via their distal, electrical, and commissural junction (E. T. Vu and F. B. Krasne, in preparation).
11. This test was impractical for recurrent inhibition because of the additional inhibition at the first synapse of the LG circuit, which prevented experimental generation of strong input to LG during recurrent inhibition.
12. C. A. Terzuolo, R. L. Purple, E. Bayly, E. Handelman, in *Structure and Function of Inhibitory Neuronal Mechanisms*, C. von Euler, S. Skoglund, U. Soderberg, Eds. (Pergamon, New York, 1968), pp. 261–289.
13. For example, lateral inhibition in sensory systems [C. Koch, T. Poggio, V. Torre, *Trends Neurosci.* **9**, 204 (1986)], or the input function rules for units in distributed networks [J. L. McClelland and D. E. Rumelhart, Eds., *Parallel Distributed Processing* (MIT Press, Cambridge, MA, 1986)].
14. The equivalent circuit in Fig. 1, which is conventional for representing excitatory chemical transmission, is also appropriate for the LG excitation via rectifying electrical junctions [D. H. Edwards, W. J. Heitler, E. M. Liese, R. A. Fricke, *J. Neurosci.* **11**, 2117 (1991)]. In Fig. 1, E_e represents the amplitude of the presynaptic spike and G_e the lumped conductances of all forward biased junctions. Although steady-state predictions are presented here, extensive modeling with a realistic compartmental model of LG and synaptic potentials that mimic observed ones give qualitatively similar predictions (E. T. Vu and F. B. Krasne, in preparation).

15. We thank M. Konishi and C. Koch for discussion and T. Teshiba for technical assistance. Supported by a predoctoral NSF fellowship to E.T.V. and by National Institute of Neurological Diseases and Stroke grant NS-08108.

11 October 1991; accepted 14 January 1992

The Size of Gating Charge in Wild-Type and Mutant *Shaker* Potassium Channels

NATHAN E. SCHOPPA, KEN MCCORMACK, MARK A. TANOUYE, FRED J. SIGWORTH*

The high sensitivity of voltage-gated ion channels to changes in membrane potential implies that the process of channel opening is accompanied by large charge movements. Previous estimates of the total charge displacement, q, have been deduced from the voltage dependence of channel activation and have ranged from 4 to 8 elementary charges (e_0). A more direct measurement of q in *Drosophila melanagaster Shaker* 29-4 potassium channels yields a q value of 12.3 e_0. A similar q value is obtained from mutated *Shaker* channels having reduced voltage sensitivity. These results can be explained by a model for channel activation in which the equilibria of voltage-dependent steps are altered in the mutant channels.

HODGKIN AND HUXLEY (*1*) NOTED that the voltage sensitivity of sodium and potassium channels requires that charges must move in response to changes in membrane potential to open the channels. Recent structure-function studies of voltage-gated channels suggest that these voltage-sensing charges are the charged amino acid residues in the fourth putative transmembrane region called S4 (*2*). The best experimental support for this claim is that mutations that neutralize these charges decrease the voltage sensitivity of the channels (*3–5*). However, some mutations in the S4 region of *Shaker* K^+ channels that do not alter the number of charges on the amino acid side chains also decrease the voltage sensitivity of activation (*4, 6*). One explanation is that mutations that do not alter charge decrease the total charge displacement by reducing the distance charged moieties move within the membrane electric field. Alternatively, these mutations may not reduce the total charge displacement at all, but may change the way in which charge displacement is coupled to channel opening. To distinguish between these two alternatives for one of these mutations, we measured the total single-channel charge displacement, q.

We compared truncated wild-type (WT) *Shaker* 29-4 channels from *Drosophila* (*7*) with truncated mutated channels (V2) in which Leu^{370}, located near the end of the S4 region, was replaced with Val (Fig. 1A) (*6, 8*). *Shaker* channels normally show rapid inactivation; that is, they open only transiently during depolarization. We used truncated channels in which residues 2 to 29 were deleted to eliminate inactivation (*9*) and allow equilibrium measurements of channel opening and gating charge. Compared to WT channels, V2 channels showed a shift of ~+40 mV in their threshold of activation (Fig. 1, B and C), consistent with shifts in nontruncated channels having this mutation (*6, 10, 11*), and also had reduced voltage sensitivity of activation (*6*).

We first obtained estimates of the total single-channel charge displacement from the voltage dependence of the channel open probability (p_o). We refer to these estimates as q_a. Given specific assumptions (*12*), p_o is proportional to $\exp(qV/kT)$, where k is the Boltzmann constant and T is the absolute temperature, at membrane potentials (V) where p_o approaches zero. Measuring p_o values between 10^{-3} and 10^{-2}, Liman and co-workers (*5*) estimated q_a to be ~7 e_0 for the rat brain (RCK1) K^+ channel. In similar measurements of q_a for the WT and V2

N. E. Schoppa, K. McCormack, F. J. Sigworth, Department of Cellular and Molecular Physiology, Yale University School of Medicine, New Haven, CT 06510.
M. A. Tanouye, Department of Entomology, University of California, Berkeley, CA 94720.

*To whom correspondence should be addressed.